METAL SITE DOPING IN THE NARROW-GAP SEMICONDUCTOR $FeGa_3$

B. KOTUR [1], V. BABIZHETSKYY [1], E. BAUER [2], F. KNEIDINGER [2], A. DANNER [2], L. LEBER [2], H. MICHOR [2]

[1] *Ivan Franko National University of Lviv, Ukraine;*

[2] *Institute of Solid State Physics, Vienna University of Technology, Austria*

The effects and feasibility of metal site doping of the tetragonal diamagnetic insulator $FeGa_3$ by Fe/Co, Fe/Mn and Co/Ni substitution were investigated by X-ray, electron probe microanalysis, electrical resistivity, specific heat and magnetic susceptibility measurements. Substitution of Fe by Co in $FeGa_3$ does not change its structure type and preserves the structure of the binary parent compound ($FeGa_3$), whereas the solubility of Mn in the $FeGa_3$ structure type is limited to 3 at.% and a finite solubility of Ni in $CoGa_3$ is not detected.

Keywords: *intermetallic compounds; homogeneity range; electron/hole doping.*

$FeGa_3$ is a diamagnetic narrow-gap semiconductor [1, 2] crystallizing in the centrosymmetric tetragonal space group $P4_2/mnm$ [3]. The related compound $CoGa_3$ is isostructural showing the same $FeGa_3$ type structure and also a diamagnetic susceptibility, however contrary to $FeGa_3$ $CoGa_3$ exhibits a metallic behaviour [3]. The opening of a semiconducting gap in intermetallic compounds such as FeSi, $FeSb_2$ or $RuAl_2$ is assumed to originate from hybridization of *p*- and *d*-states. In the case of $FeGa_3$ additional effects become relevant which are related to specific features of the crystal structure displayed in Fig. 1. The basic structure building element are 3^2434 nets formed by one kind of Ga atoms and pairs of Fe atoms (dimers). Stacking 3^2434 nets on top of each other generates rows of Ga_8 cubes (black) and Ga_6 doubled rhombic prisms with one shared face. The cubes are centred by the second kind of Ga atoms; the doubled trigonal prisms formed by Ga are occupied by Fe–Fe dimers (gray circles). The electronic structure of $FeGa_3$ was studied by several research groups by means of ab-initio calculations [3–5] as well as experimentally by photoemission spectroscopy [6]. Calculations based on the local density approximation (LDA) suggest the electronic density of states (EDOS) to be dominated by parabolically distributed, nearly free electron like states with *s-p* bands from the Ga network at low energies and hybridized Fe *d*- and Ga *p*-states at higher energies leading to a narrow band gap (~0.3 eV) in this compound [3, 4]. Based on extended LDA calculations which include on-site Coulomb repulsion (LDA + U) Yin and Pickett [5] discussed the formation of antialigned moments at the Fe_2 dimers with a band gap at moderate values of the Coulomb repulsion U ~2 eV. For higher values of U they obtained an unrealistic metallic state. Such a metallic state, however, is reported for $CoGa_3$ which is also diamagnetic and crystallizes in the same centrosymmetric tetragonal space group $P4_2/mnm$ [7] and a metal-insulator (MI) transition has been reported for the solid solution $(Fe,Co)Ga_3$ for the composition $Fe_{0.95}Co_{0.05}Ga_3$ [2].

In the present paper we investigate the solid solutions $Fe_{1-x}Co_xGa_3$ (a conference report was presented earlier [8]) as well as the possible formation of $Fe_{1-x}Mn_xGa_3$ and $Co_{1-x}Ni_xGa_3$ and study the evolution of magnetism in these systems. In the course of manuscript preparation we noticed that similar studies on electron doping of $FeGa_3$ were

Corresponding author: B. KOTUR, e-mail: kotur@franko.lviv.ua

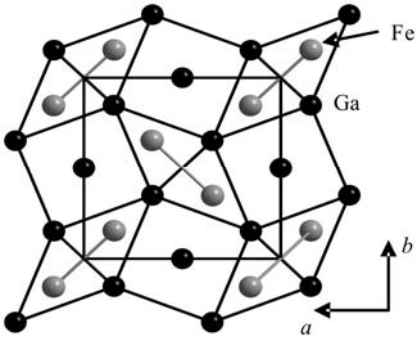

Fig. 1. Crystal structure of $FeGa_3$ along [0 0 1].

carried out parallel to our work by the group of Takabatake and recently published in [9]. In addition to results on $Fe_{1-x}Co_xGa_3$, they report on a ferromagnetic instability occurring in the solid solution $FeGa_{3-x}Ge_x$.

Experimental. The ternary alloys $Fe_{1-x}Co_xGa_3$ and $Fe_{1-x}Mn_xGa_3$ as well as binary $CoGa_3$ and $FeGa_3$ were prepared in different ways from mixtures of the pure elements: Mn powder (Strem Chemicals, 99.99%), powders of Fe, Co and Ni (all Johnson Matthey, 99.99%), and Ga rod (Ingal, 99.9999%). The series consisted of stoichiometric mixtures with the compositions $Fe_{1-x}Co_xGa_3$ (x = 0; 0.05; 0.15; 0.25; 0.5; 0.75; 1), $Fe_{1-x}Mn_xGa_3$ (x = 0; 0.05; 0.1; 0.4) and $Co_{1-x}Ni_xGa_3$ (x = 0; 0.05; 0.1; 0.25). The reactants were carefully mixed, pressed into pellets, and loaded into quartz glass ampoules, which were sealed under vacuum (approx 10^{-5} mbar). All samples were heated to 800°C at the rate of 200°C/h, held at this temperature for 24 h, and finally cooled to room temperature at the rate of 20°C/h. Excess Ga by the synthesis of single crystals of $CoGa_3$ was dissolved with 3M HCl and the remains were washed with deionized water. The products consisting of well-shaped, silvery-gray crystals (with sizes up to 1 mm) were characterized by the X-ray powder diffraction.

X-ray powder diffraction patterns for the full profile refinement of the binary and ternary samples were collected on a Siemens D5000 powder diffractometer with monochromated CuK_α radiation ($18° \le 2\theta \le 82°$, step size 0.02°, measurement time per step: 3 s) and on a powder diffractometer STOE STADI P with monochromated $MoK_{\alpha 1}$ radiation ($8° \le 2\theta \le 65°$, step size 0.1°, measurement time per step: 150 s).

Energy dispersive X-ray spectroscopy analysis (EDX) of the polished samples by a scanning electron microscope (TESCAN 5130MM with Oxford Si-detector) confirmed the presence of only iron and/or cobalt and gallium. The nominal overall composition measured by EDX corresponds to the samples composition and shows no deviation from the starting composition.

Zero-field heat capacity measurements in the temperature range 0.4...20 K were carried out with a relaxation method in a ^{3}He Quantum Design PPMS calorimeter with a careful addenda calibration using synthetic α-Al_2O_3 (NIST reference material № 720). Additional heat capacity measurements up to room temperature were performed with a standard ^{4}He PPMS calorimeter. Magnetic measurements were performed on a CRYOGENIC SQUID magnetometer (3 K to room temperature) in various fields up to 6 T. The temperature dependence of the electrical resistivity was studied on the bar shaped pressed powder samples with spot welded Au-contacts via a four probe a.c. method in the temperature range 4...300 K.

Results and discussion. ***Phase formation and structural characterization.*** Earlier, the crystal structure of $CoGa_3$ was designated with the non-centrosymmetric space group P-4n2 ($CoGa_3$ type structure) [10, 11]. As it was indicated by Pöttgen [12] deviations of the atomic coordinates in these two structure types $FeGa_3$ and $CoGa_3$ are negligible and they can not be distinguished by the powder X-ray diffraction analysis. The single crystal XRD data [6] confirmed the centrosymmetric space group $P4_2/mnm$ for the whole range of the $Fe_{1-x}Co_xGa_3$ solid solution.

X-ray diffraction (XRD) patterns of polycrystalline $FeGa_3$ as well as Co- and Mn-doped samples of $FeGa_3$ are presented in Figs. 2 and 3. Substitution of Fe by Co or Mn in $FeGa_3$ does not change its structure. The unit cell parameters for $Fe_{1-x}Co_xGa_3$ (x = 0; 0.05; 0.25; 0.5; 0.75; 1) and $Fe_{1-x}Mn_xGa_3$ (x = 0.05; 0.1; 0.4) are presented in Table 1.

The XRD patterns obtained from all Co-doped samples indicate homogeneous phases of $FeGa_3$ without impurity peaks from the elemental or secondary phases. Refined lattice parameters of the parent compounds are in good agreement with data reported previously [1, 3, 4]. The substitution of Fe by Co leads to a linear increase of the unit cell volume (compare Table 1). A substitution of Fe by Mn occurs only on quantity of about 5 at.% and leads to the change of cell parameters as well as peaks intensities (see Fig. 3). Compounds with the $FeGa_3$ structure type are formed exclusively between a transition metal from either the Fe or Co group and one of the 3b element Ga and In.

Table 1. Unit cell parameters (XRD powder data) for $Fe_{1-x}Co_xGa_3$ (x = 0; 0.05; 0.25; 0.5; 0.75; 1) and $Fe_{1-x}Mn_xGa_3$ (x = 0.05; 0.1; 0.4)

Composition	a [Å]	c [Å]	V [Å^3]
$CoGa_3$	6.2374(5)	6.4379(1)	250.47(5)
$Fe_{0.25}Co_{0.75}Ga_3$	6.2490(4)	6.4624(9)	252.34(6)
$Fe_{0.50}Co_{0.50}Ga_3$	6.2639(3)	6.5006(5)	255.06(4)
$Fe_{0.75}Co_{0.25}Ga_3$	6.2622(6)	6.5358(6)	256.28(9)
$Fe_{0.95}Co_{0.05}Ga_3$	6.2685(3)	6.5587(7)	257.70(5)
$FeGa_3$	6.268(1)	6.560(1)	257.7(2)
$Fe_{0.95}Mn_{0.05}Ga_3$	6.2715(3)	6.5721(6)	258.49(5)
$Fe_{0.90}Mn_{0.1}Ga_3$	6.2720(4)	6.5714(6)	258.50(6)
$Fe_{0.60}Mn_{0.4}Ga_3$*	6.2713(2)	6.5737(4)	258.54(4)

* two phase region.

The eight representatives are known: $FeGa_3$; $RuGa_3$; $OsGa_3$; $CoGa_3$; $RuIn_3$; $CoIn_3$; $RhIn_3$; $IrIn_3$. The electron count or valence electron concentration (VEC, number of valence electrons per formula unit) is limited to a range between 17 and 18 electrons.

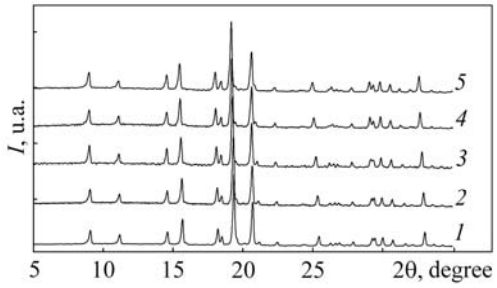

Fig. 2.

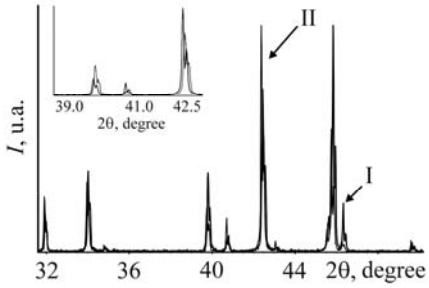

Fig. 3.

Fig. 2. X-ray diffraction patterns ($MoK_{\alpha 1}$ radiation) of polycrystalline pseudo-binary alloys $Fe_{1-x}Co_xGa_3$ (x = 0; 0.25; 0.5; 0.75; 1). *1* – $CoGa_3$; *2* – $Co_{0.75}Fe_{0,25}Ga_3$; *3* – $Co_{0.50}Fe_{0,50}Ga_3$; *4* – $Co_{0.25}Fe_{0,75}Ga_3$; *5* – $FeGa_3$.

Fig. 3. X-ray diffraction patterns (CuK_{α} radiation) of polycrystalline pseudo-binary alloys $Fe_{1-x}Mn_xGa_3$ (x = 0; 0.1). I – $Fe_{0.9}Mn_{0.1}Ga_3$; II – $FeGa_3$.

This indicates that compounds with the $FeGa_3$ structure are intermetallic electron compounds. The occurrence of the structure type is governed primarily by the electron count because the band energy term of the total energy determines the structural stability [3]. So, the substitution of Fe by Co in the $FeGa_3$ structure reveals a small difference of atomic radii (r_{Fe} = 1.26 Å; r_{Co} = 1.25Å) and changes the VEC to 18 for $CoGa_3$. Our attempts to substitute Co by Ni (r_{Ni} = 1.24Å) in the $CoGa_3$ structure were not successful

and in agreement with VEC concept. Contrary to them the substitution of Fe by Mn in the $FeGa_3$ structure has a limit of about 5 at.%. There is a larger difference of atomic radii between Fe and Mn (r_{Mn} = 1.35Å). The VEC limit for stability of compounds with the $FeGa_3$ structure is not strict and may have a small tolerance to below 17 as in case of $Fe_{1-x}Mn_xGa_3$ ($0 \le x \le 0.1$).

Physical properties. The temperature dependent magnetic susceptibility M/H and inverse susceptibility H/M of pseudo-binary solid solutions $Fe_{1-x}Co_xGa_3$ measured in a field of 3T are displayed in Figs 4. While the binary parent compounds (not shown in Fig. 4) are diamagnetic [2], all pseudo-binaries are clearly paramagnetic with a Curie–Weiss type susceptibility at high temperatures together with a negligible small temperature independent Pauli susceptibility $\tilde{\chi}_0$. Thus, analyzing the data in terms of a simple Curie–Weiss law, $\chi = C/(T - \Theta_P)$, with $C = N_A\mu_0\mu_{eff}^2/3k_B$ being the Curie constant and Θ_P the paramagnetic Curie temperature reveals a roughly linear increase of Θ_P and super-linear increase of the effective paramagnetic moment μ_{eff} with increasing Fe content from μ_{eff} = 0.29 μ_B/f.u. for $Fe_{0.25}Co_{0.75}Ga_3$, to 0.73 μ_B/f.u. for $Fe_{0.5}Co_{0.5}Ga_3$ to finally μ_{eff} = 1.53 μ_B/f.u. for $Fe_{0.75}Co_{0.25}Ga_3$. For the pseudo-binary compound right at the MI transition, $Fe_{0.95}Co_{0.05}Ga_3$, Bittar et al. [2] reported an effective moment of only 0.155 μ_B/f.u. indicating a dramatic collapse of the 3*d* moment in the close vicinity of the binary parent compound $FeGa_3$. All data are presented in Table 2 and Fig. 6*a*.

The temperature dependent specific heat of selected pseudo-binaries $Fe_{1-x}Co_xGa_3$ is shown in Fig. 5 as C/T vs. T^2, an increase of the Sommerfeld coefficient γ is revealed from about 3 mJ/(mol·K^2) for $CoGa_3$ to about 17 mJ/(mol·K^2) when reaching $Fe_{0.75}Co_{0.25}Ga_3$ (see Fig. 6*b*). Again (in analogy to the effective paramagnetic moment) the electronic contribution drops at the Fe-rich side where Bittar et al. [2] reported γ = 6.3 mJ/(mol·K^2) for $Fe_{0.95}Co_{0.05}Ga_3$ and finally a negligible T-linear specific heat contribution (0.03 mJ/(mol·K^2) for $FeGa_3$.

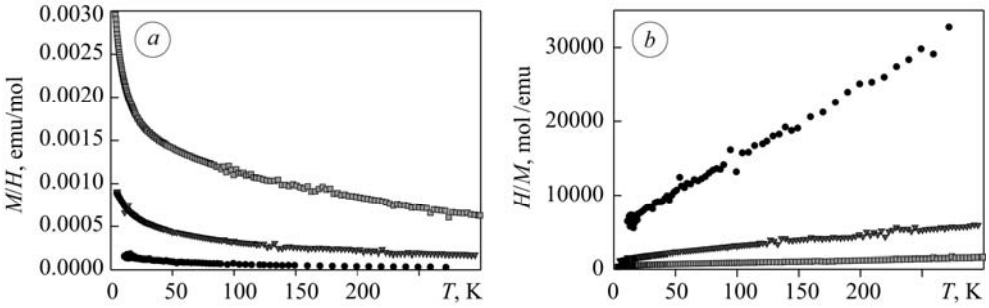

Fig. 4. The temperature dependent static susceptibility M/H (*a*: ● – $Co_{0.75}Fe_{0.25}Ga_3$; ▼ – $Co_{0.5}Fe_{0.5}Ga_3$; ■ – $Co_{0.25}Fe_{0.75}Ga_3$) and inverse susceptibility H/M (*b*: ● – $Co_{0.25}Fe_{0.75}Ga_3$; ▼ – $Co_{0.5}Fe_{0.5}Ga_3$; ■ – $Co_{0.75}Fe_{0.25}Ga_3$) of various compositions of the solid solution $Fe_{1-x}Co_xGa_3$ measured at 3T.

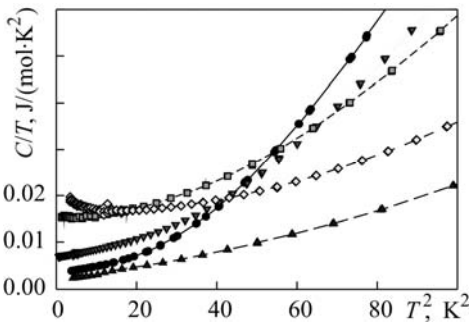

Fig. 5. The temperature dependent low temperature specific heat represented as C/T vs. T^2 of solid solutions $Fe_{1-x}Co_xGa_3$ as labelled. ● – $CoGa_3$; ▼ – $Co_{0.75}Fe_{0.25}Ga_3$; ■ – $Co_{0.5}Fe_{0.5}Ga_3$; ◆ – $Co_{0.25}Fe_{0.75}Ga_3$; ▲ – $FeGa_3$.

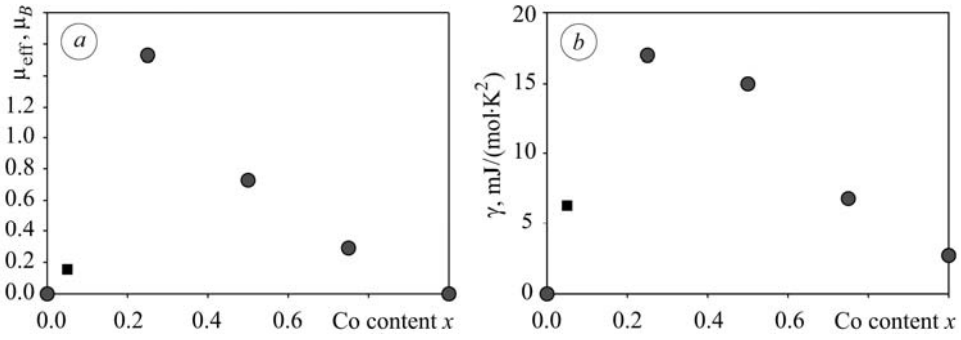

Fig. 6. Dependence of the effective magnetic moment μ_{eff} (*a*) and the Sommerfeld coefficient of the electronic specific heat γ (*b*) on the Co content *x* in $Fe_{1-x}Co_xGa_3$. The square symbol ■ refers to data for $x = 0.05$ [2].

Table 2. Paramagnetic Curie temperatures, θ_P, and effective magnetic moments, μ_{eff}, of pseudo-binaries $Fe_{1-x}Co_xGa_3$ obtained from Curie–Weiss fits (data for $x = 0.05$ [2])

Composition	θ_P, K	μ_{eff}, μ_B	comment
$CoGa_3$	–	–	diamagnetic
$Fe_{0.25}Co_{0.75}Ga_3$	–60	0.29	–
$Fe_{0.50}Co_{0.50}Ga_3$	–106	0.73	–
$Fe_{0.75}Co_{0.25}Ga_3$	–153	1.53	–
$Fe_{0.95}Co_{0.05}Ga_3$	–1.5	0.155	*Ref. [2]
$FeGa_3$	–	–	diamagnetic

The temperature dependent electrical resistivity data displayed in Fig. 7 exhibit a metallic-like behaviour for all alloys $Fe_{1-x}Co_xGa_3$ (with $x < 0.8$) and a systematic increase of the electrical resistivity with decreasing Co content *x*. Electron doping, accordingly, results in a filling of conduction band states and simultaneous formation of local magnetic moments at the (Fe, Co)–(Fe, Co) dimers. Mixing two different species d-metal ions with presumably different magnetic moments is incompatible with respect to the formation of a singlet state on these dimers. We note that very similar results of magnetic susceptibility, specific heat and electrical resistivity were recently reported from a study based on single crystalline samples with a slightly different set of compositions $Fe_{1-x}Co_xGa_3$ [9].

The initial effects of hole doping, i.e. the substitution of Fe by Mn, can be evaluated only from the alloys with smallest Mn concentration, $Fe_{0.95}Mn_{0.05}Ga_3$, for which a small but finite increase of the unit cell volume is revealed by X-ray diffraction (see section 3.1). Temperature and field dependent magnetisation studies of $Fe_{0.95}Mn_{0.05}Ga_3$ reveal contributions from a ferromagnetic component with a Curie temperature T_C of about 160 K and a very small saturation moment of $6.2 \cdot 10^{-3}$ μ_B/f.u. which seems to be of extrinsic origin. When subtracting this ferromagnetic contribution from the temperature dependent

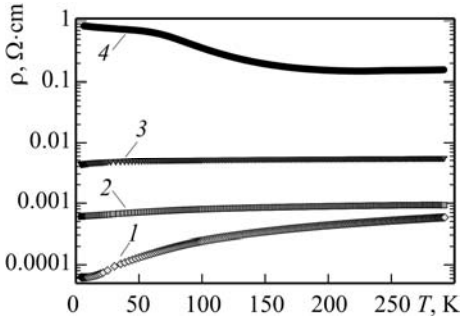

Fig. 7. The temperature dependent electrical resistivity of pseudo-binaries $Fe_{1-x}Co_xGa_3$ as labelled: *1* – $Fe_{0.5}Co_{0.5}Ga_3$; *2* – $Fe_{0.75}Co_{0.25}Ga_3$; *3* – $CoGa_3$; *4* – $FeGa_3$.

magnetisation data measured at 3 T and 5 T we obtain a reasonable scaling of the corresponding inverse susceptibility data $H/M = 1/\chi$ shown in Fig. 8*a* in the temperature range up to 150 K (i.e. below the ordering temperature of the ferromagnetic impurity). Analysing these data for a temperature range 40...150 K in a similar fashion as for solid solutions $Fe_{1-x}Co_xGa_3$ in terms of a simple Curie–Weiss law, $\chi = C/(T-\Theta_P)$ (see above), we obtain for $Fe_{0.95}Mn_{0.05}Ga_3$ a negative paramagnetic Curie temperature $\Theta_P = -60$ K, a Curie constant $C = 0.152$ (emu·K)/mol and accordingly an effective magnetic moment $\mu_{eff} = 1.1\ \mu_B$/f.u. which is far larger that the effective moment induced by the corresponding amount of Co substitution in $Fe_{0.95}Co_{0.05}Ga_3$. The low temperature specific heat data of $Fe_{0.95}Mn_{0.05}Ga_3$ displayed as C/T vs. T^2 in Fig. 8*b* further reveals a marked difference between Co and Mn substitution. While in the case of Co substitution the conduction band states are filled by the extra electron and accordingly a rather large T-linear Sommerfeld contribution is observed (see above), there is hardly any T-linear component visible in the specific heat of $Fe_{0.95}Co_{0.05}Ga_3$ in Fig. 8*b*. There is rather a significant magnetic contribution which may origin from spin-glass like correlations or other low energy magnetic excitations. The absence of a T-linear electronic specific heat contribution indicates that hole doping of the valence band is hardly possible which is also corroborated by the rather low solubility of Mn in $FeGa_3$.

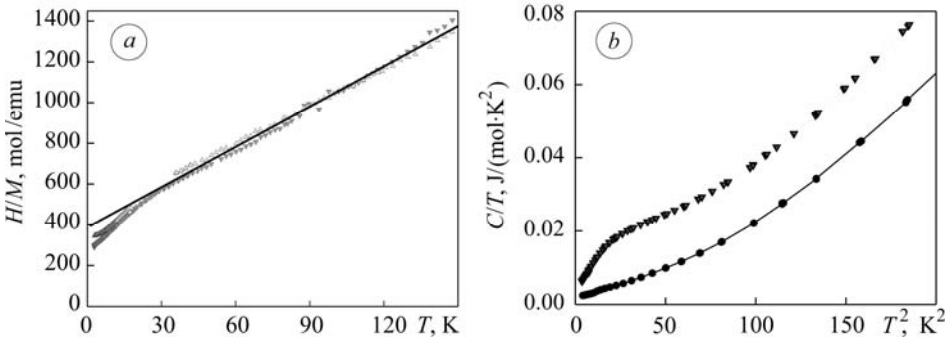

Fig. 8. Temperature dependent inverse susceptibility H/M of $Fe_{0.95}Mn_{0.05}Ga_3$ (*a*: ▼ – 3T; ▲ – 5T) and low temperature specific heat C/T vs. T^2 of $Fe_{0.95}Mn_{0.05}Ga_3$ and $FeGa_3$ (*b*: ● – $FeGa_3$; ▼ – $Fe_{0.95}Mn_{0.05}Ga_3$).

CONCLUSIONS

A complete solid solution while preserving the tetragonal $P4_2/mnm$ crystal structure is possible for (Fe, Co)Ga_3, whereas the solubility of Mn in the $FeGa_3$ structure is limited to about 3 at.%; a finite solubility of Ni in $CoGa_3$ is not detected. Electron doping via the substitution of Fe by Co in the diamagnetic narrow-gap semiconductor $FeGa_3$ reveals the appearance of a metallic conducting state which – together with the observation of a significant electronic specific heat contribution – indicates a gradual filling of conduction band states by the extra d-electrons donated by Co atoms. The occurrence of a distinct Curie–Weiss-type local moment paramagnetism may be related to magnetic moments forming at mixed Fe/Co dimers, while $FeGa_3$ as well as $CoGa_3$ are both diamagnetic irrespective of their semiconducting or metallic ground states. An analogous substitution of Fe by Mn, in particular $Fe_{0.05}Mn_{0.05}Ga_3$, indicates that the semiconducting state of $FeGa_3$ remains intact, while the magnetic state of Fe–Fe dimers seems to be strongly affected by the small amount of Mn atoms dissolved in the lattice, thus, leading to a Curie–Weiss type paramagnetism even at very small Mn concentrations.

РЕЗЮМЕ. Методами рентгенівського, мікрорентгеноспектрального аналізу, дослідження електроопору, питомої теплоємності і магнетної сприйнятливості вивчено можливість та вплив легування Fe/Co, Fe/Mn і Co/Ni у положеннях атомів металу в тетрагональній структурі діамагнетного ізолятора $FeGa_3$. Заміщення атомів Fe на Co у сполуці $FeGa_3$

не змінює її кристалічну структуру. Розчинність Mn у $FeGa_3$ не перевищує 3 at.%, а розчинність Ni у $CoGa_3$ не виявлено.

РЕЗЮМЕ. Методами рентгеновского, микрорентгеноспектрального анализа, исследования электросопротивления, удельной теплоемкости и магнитной восприимчивости исследована возможность и влияние легирования Fe/Co, Fe/Mn и Co/Ni в положениях атомов металла в тетрагональной структуре диамагнитного изолятора $FeGa_3$. Замещение атомов Fe на Co в соединении $FeGa_3$ не изменяет ее кристаллическую структуру. Растворимость Mn в $FeGa_3$ не превышает 3 at.%, а растворимость Ni в $CoGa_3$ не выявлено.

Acknowledgement. This work was supported by the Ukrainian–Austrian WTZ project №UA-5/2011.

1. *Thermoelectric* properties of semiconductorlike intermetallic compounds $TMGa_3$ (TM = Fe, Ru, and Os) / Y. Amagai, A. Yamamoto, T. Iida, and Y. Takanashi // J. Appl. Phys. – 2004. – **96**. – P. 5644–5648.
2. *Correlation* effects in the small gap semiconductor $FeGa_3$ / E. M. Bittar, C. Capan, G. Seyfarth, P. G. Pagliuso, and Z. Fisk // J. Phys.: Conf. Ser. – 2010. – **200**. – P. 012–014.
3. *$FeGa_3$* and $RuGa_3$: semiconducting intermetallic compound / U. Häussermann, M. Boström, P. Viklund, Ö. Rapp, T. Björnängen // J. Solid State Chem. – 2002. – **165**. – P. 94–99.
4. *Imai Y. and Watanabe A.* Electronic structures of semiconducting $FeGa_3$, $RuGa_3$, $OsGa_3$, and $RuIn_3$ – of the $FeGa_3$-type structure// Intermetallics. – 2006. – **14**. – P. 722–728.
5. *Yin Z. P. and Pickett W. E.* Evidence for a spin singlet state in the intermetallic semiconductor $FeGa_3$ // Phys. Rev. B. – 2010. – **82**. – P. 155–202.
6. *Electronic* structure of a narro-gap semiconductor $FaGa_3$ investigated by photoemission and inverse photoemission spectroscopies / M. Arita, K. Shimada, Y. Utsumi et al. // Phys. Rev. B. – 2011. – **83**. – 245116.
7. *Variations* of the $FeGa_3$ structure type in the systems $CoIn_{3-x}Zn_x$ and $CoGa_{3-x}Zn_x$ / P. Viklund, S. Lidin, P. Berastegui, U. Häussermann // J. Solid State Chem. – 2002. – **165**. – P. 100–110.
8. *Evolution* of magnetic correlations in the solid solution $Co_{1-x}Fe_xGa_3$ / H. Michor, V. Babizhetskyy, E. Bauer, et al. // SCTE 2012. 18th Int. Conf. on Solid Compounds of Transition Elements. Lisboa, 31st March–5th April 2012. – P. 203.
9. *Ferromagnetic* instability in a doped band gap semiconductor $FeGa_3$ / K. Umeo, Y. Hadano, S. Narazu, et al. // Phys. Rev. B. – 2012. – **86**. – P. 144–421.
10. *Zum* Aufbau der Systeme Kobalt-Gallium, Palladium-Gallium und verwandter Legierungen / K. Schubert, H. L. Lukas, H.-G. Meissner, S. Bhan // Z. Metallk. – 1959. – **50**. – S. 534–539.
11. *Dasarathy C. and Hume-Rothery W.* The system Iron-Gallium // Proc. R. Soc. – London, Ser. A. – 1965. – **286**. – P. 141.
12. *Pöttgen R.* Preparation, crystal structure and properties of $RuIn_3$ // J. Alloys Compd. – 1995. – **226**. – P. 59–64.

Received 04.12.2012